A NEW METHOD FOR HARDNESS CALCULATION USING INSTRUMENTED INDENTATION TESTING

G. Pintaúde
Academic Department of Mechanical, CEFET – PR, Curitiba Branch, Av. Sete de Setembro, 3165, Curitiba – PR.
e-mail: pintaude@cefetpr.br

A. Sinatora
Mechanical Engineering Department, USP, Av. Prof. Mello de Moraes, 2231, São Paulo – SP.
e-mail: sinatora@usp.br

Instrumented indentation testing (IIT) is a potential technique to determine materials properties as hardness, elastic modulus and, in some cases, fracture toughness and work-hardening coefficient. This paper presents a review of the current analysis for IIT and the reasons for their limitations. Moreover, it is presented, for some testing conditions, a new methodology to calculate a "true hardness" (H_{IP}), using at the same time IIT curves and the measurements of indentation areas, resulting in a factor called α. Experimental tests were carried out using Vickers indenter and hardness measurements were made on a glass and on bearing steel. H_{IP} calculation is able to incorporate the indentation morphology, which depends on the processes during the loading step and can be estimated from the α value. Three different proposals of analysis for mechanical behavior of materials during an indentation are discussed, as well as the potentials and limitations of the new method for hardness calculation. A practical application for H_{IP} concept is related to the transition between abrasive wear regimes, mild to severe, which depends on the abrasive-to-worn material hardness ratio. The use of H_{IP} concept allows correlating the phenomena that occur in abrasive process with those observed in indentation testing.

Key words: hardness; elastic modulus; instrumented indentation testing; abrasive wear.

1. Introduction

Frölich et al. (1977) presented the instrumented indentation testing (IIT) as a potential technique to determine materials properties in addition to the conventional hardness. These researches presented a method to calculate a hardness value that is not affected by size effect, using the microscopic range of loads. Further, this technique became in a major way to determine the mechanical properties of coatings, and the equipments were developed to operate in the nanoscopic range of loads. Since 1993 it has been concentrated efforts to publish an standard to define the properties obtained from IIT. The main quantities defined in the ISO/FDIS 14577-1 (2002) are presented in the following equations.

1) Based on the Wilde and Wehrstedt (2001) paper, ISO/FDIS 14577-1 Standard (2002) defined Martens hardness (HM)[(1)] [N/mm^2], as shown in equation 1:

$$HM = \frac{F_{máx}}{A_S} = \frac{F_{máx}}{k\ h_{máx}^{\ 2}} \tag{1}$$

where,
A_S is the superficial area;
h_{max} is the maximum depth at maximum load;
k is a geometric factor (26,43 for Vickers indenter).

2) Indentation hardness (H_{IT}) [N/mm^2] is defined as the maximum force divided by the projected area of contact (A_P) between the indenter and the tested material, as shown equation 2 :

$$\mathrm{H_{IT}} = F_{máx} / A_P = F_{máx} / 24{,}5.\mathrm{h_C}^2 \tag{2}$$

[1] Until 2001 it was called *Universal hardness (HU)* (WEILER, 1989).

where,
A_P is the projected area [mm^2] (= $24.5.h_C^2$ for Vickers indenter) and;
h_C is the contact depth.

In equation 2 it is presented the h_C quantity, called contact depth. There is more than one methodology to determine this depth, and these proposals will be presented in the next item. The well-know method to determine it is presented in Figure 1.

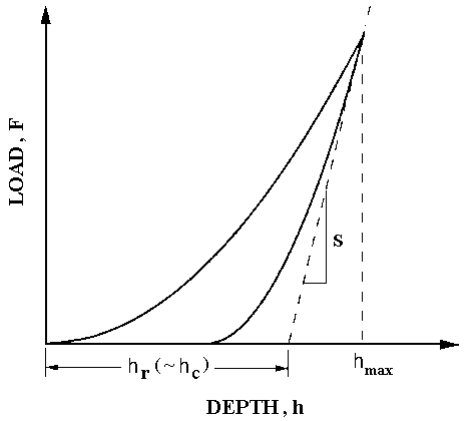

Figure 1. Typical curve obtained from instrumented indentation testing (ISO/FDIS 14577-1; ISO, 2002), indicating the h_r (intersection with the X axis) and contact stiffness S [N/mm].

3) Indentation modulus (E_{IT}) – [N/mm^2]: to calculate this quantity it is necessary to know the reduced elastic modulus concept, as shown in equation 3:

$$\frac{1}{E_r} = \frac{1-\nu_i^2}{E_i} + \frac{1-\nu^2}{E} \tag{3}$$

where,
E_r is the reduced elastic modulus [GPa];
E_i is the elastic modulus of indenter (1,140 GPa [2]);
ν_i is the Poisson ratio of indenter (0.07 [2]);
E is the elastic modulus of tested material [3] [GPa] and;
ν is the Poisson ratio of tested material.

An expression for reduced elastic modulus E_r (equation 3) calculation is presented in equation 4:

$$E_r = \frac{S}{\beta\sqrt{A_P}} \tag{4}$$

where,
β is a geometric factor (= 1.142 for Vickers indenter: King, 1987) and;
S is the contact stiffness [N/mm] (defined in Fig. 1).

[2] Adopted values by ISO/FDIS 14577-1 (ISO, 2002).
[3] $E/(1-\nu^2)$ was denominated by ISO/FDIS 14577-1 (ISO, 2002) as "*indentation modulus*", using E_{IT} symbol.

2. Analysis of load vs. depth penetration curves

Two methodologies for the calculation of contact stiffness by means of the tangent to unloading curve are well known. The first is due to Doerner and Nix (1986), whose proposed the *linear extrapolation method* (LEM), which supposes that around 30% of unloading curve can be approximated by linear behavior.
The second methodology was proposed by Oliver and Pharr (1992), known as *potential law method* (PLM), which consider that the first part of curve is not linear and can be described by means of potential equation, as shown in equation 5:

$$F = C_{UL}(h - h_P)^{m_{UL}} \tag{5}$$

where,
C_{UL}, m_{UL} are constants that depend on the tested material.

The contact stiffness value results from the derivation of equation 5 in function of h depth (dF/dh), as shown in equation 6:

$$S = C_{UL}\, m_{UL}(h_{máx} - h_P)^{m_{UL}-1} \tag{6}$$

In addition, Oliver and Pharr proposed that the intersection of tangent line to the X axis, which determines the h_r value, can be used to define the contact depth, h_C, as shown the equation 7:

$$h_C = h_{máx} - \varepsilon(h_{máx} - h_r) \tag{7}$$

where,
ε is a geometric factor (= 0,75 for Vickers indenter: Oliver and Pharr, 1992).

An important phenomenon observed in indentation process is the pilling-up and sinking-in morphologies. These effects are related to elasto-plastic properties of materials and the aspect of them can be observed in Figure 2.

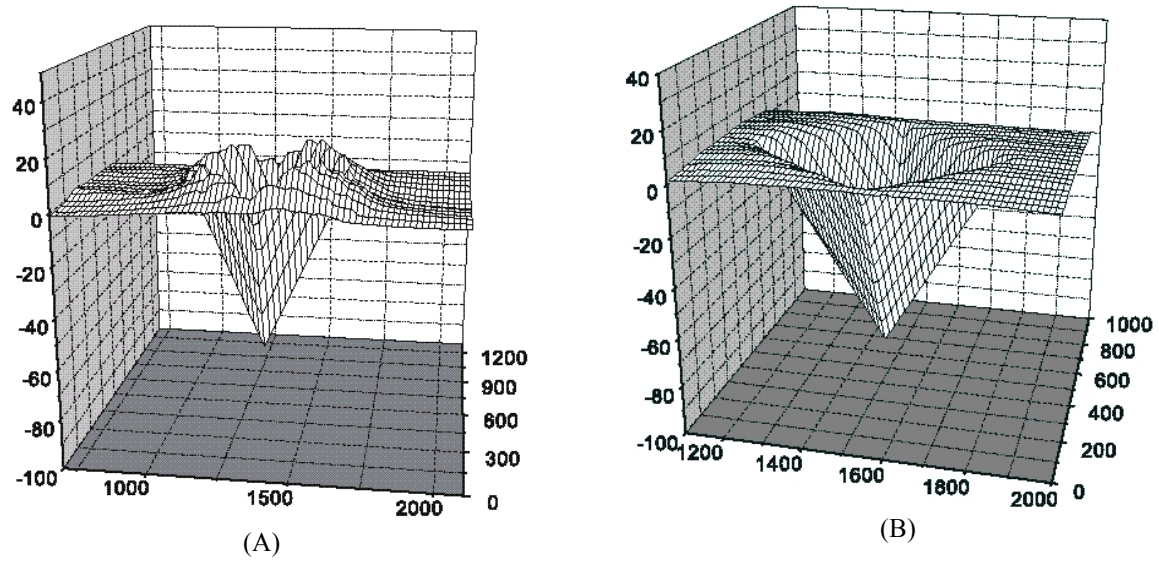

Figure 2. A) Pilling-up indentation morphology after test using load of 160 N on work-hardened copper and B) sinking-in indentation morphologie after test using load of 100 N on annealed copper (Alcala et al., 2000).

PLM has been contested by other researches (Zeng et al., 1996; Giannakopoulos and Suresh, 1999; Alcalá et al., 2000 and Strange and Varshneya, 2001), because it defines the h_C depth from the unloading curve, while this quantity is physically defined during the loading step. In this way, in the cases of pilling-up occurrence, H_{IT} and E_r values may be inadequate when they are calculated by PLM, because contact depth will be larger than the maximum depth, as shown in Figure 3.

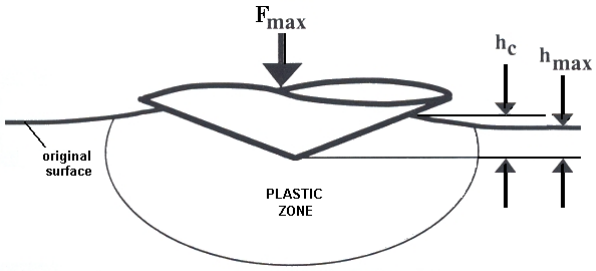

Figure 3. Plastic zone magnitude, observed in the case of pilling-up occurrence (CSM Instruments, 2002).

Zeng et al. (1996) proposed the equation 8 to calculate the h_C depth:

$$h_c = h_{máx} / \alpha^{1/2} \quad (8)$$

This equation incorporate the effects resulting from the indentation morphologies, as pilling-up and sinking-in, which are considered by means of α factor, which can be determined as indicated in equation 9:

$$\alpha = \frac{24{,}5.h_{máx}^{\ 2}}{d^2/1{,}854} \quad (9)$$

Following Zeng et al. (1996), α values smaller than 1 means pilling-up occurrence, while values larger than the unity indicates sinking-in occurrence. Zeng et al. compared for ceramic materials the h_C values obtained from equation 8 with those calculated by PLM and the differences were about 20%. Using equation 8, Zeng et al. proposed that the projected area calculated with maximum depth, h_{max}, instead of contact depth, h_C, would determine the indentation modulus. Strange and Varshneya (2001) applied this concept to indentation tests with 6061-T6 aluminum alloy (pilling-up was observed) and found an indentation modulus value 20% smaller than that calculated using PLM.
The literature shows other proposals to calculate α factor. One of them is due to Giannakopoulos and Suresh (1999), whose defined this factor as (h_P / h_{max}) ratio, i.e., the final depth after unloading and the maximum depth penetration. In this definition, pilling-up may be occur when α value is larger than 0.875. Finally, Alcalá et al. (2000) proposed a definition to α factor as shown in equation 10:

$$\alpha = (h_C / h_S)^2 \quad (10)$$

where,
h_C is the contact depth; and
h_S is the deflected depth (= h_{max} - h_C).
The use of equation 10 implies that pilling-up may be observed when ($\alpha^{1/2} - 1$) is larger than zero.

This paper present a new methodology to determine the materials hardness using IIT, based on the Zeng et al. (1996) proposal for α factor, which express pilling-up or sinking-in occurrences.

3. Materials and methods

Two types of steel were tested: AISI 1006 e AISI 52100. The carbon content of AISI 1006 steel is 0.07% and this material was tested in as-cast condition. AISI 52100 steel was treated at 900 °C by 1 h and oil-quenched. This steel was tested in different metallurgical conditions:

- Annealed;
- Wire-drawing; and
- Quenched and tempered at 500 °C by 24 h.

The chemical composition of AISI 52100 steel is presented in Table 1.

Table 1. Chemical composition of AISI 52100 steel (% mass).

C	Mn	Si	Cr	Ni	Mo	S	P
1.03	0.39	0.29	1.49	0.14	0.05	0.01	0.02

In addition, the grains of an abrasive coated paper (glass) were tested on IIT.

The equipment used to measure hardness is a Fisher H 100 XYPROG tester. During the hardness tests, load-indentation depth-time data were recorded as a Vickers indenter was driven into the sample (loading segment) and then withdrawn from it (unloading segment). A maximum test load of 1000 mN was applied in 60 steps and the hold time at each step was 0.1 s. The loading/unloading rate of the indenter was 3.6 mN/s.

The instrumented indentation testing procedure was:
- Selection of maximum depth penetration, and application of loading in 60 steps of 0.1 s for each one;
- After maximum force be reached, it was kept constant by 10 s;
- Unloading was made using 100 steps of 0.1 s each one, until a load of 0.4 mN be reached.

The maximum depth penetration was selected after roughness measurement of worn surface. Abrasive wear tests were conducted in the referred materials, reported previously (Pintaúde et al., 2001a), using average grain size of 0.2 mm. The roughness parameter Rz was used as criterion to select the maximum depth penetration. For the tested materials this value it was around 3 μm. It is important to remark that all hardness measurements were performed on polished surfaces.
In order to determine the size of indentation marks, the optical system of a conventional hardness testing was used. The average values correspond to seven measurements.

4. Proposal of hardness calculation: true hardness concept

Using the α factor suggested by Zeng et al. (1996) presented in equation 9, a new concept to hardness calculation it will be proposed. The following equations show the development used to achieve the 'true hardness' concept.

$$H_{IP} = \frac{F_{máx}}{A_{true}} = \frac{F_{máx}}{C'.h_C^{\,2}} = \frac{F_{máx}.\alpha}{C'.h_{máx}^{\,2}} \tag{11}$$

$$\alpha = \frac{A_{ideal}}{A_{true}} = \frac{24{,}5.h_C^{\,2}}{C'.h_C^{\,2}} = \frac{24{,}5}{C'} \tag{12}$$

$$H_{IP} = \frac{F_{máx}.\alpha^2}{24{,}5.h_{máx}^{\,2}} \tag{13}$$

$$A_{true} = 24{,}5\,(h_{máx}/\alpha)^2 \tag{14}$$

where,
C' is a constant relating the applied force to the square of depth during the loading step [MPa].

A significative difference can be observed between equation 14 (A_{true}) and the definitions of contact area presented in equations 1 and 2 (A_S and A_P).

5. Results and discussion

Table 2 presents the maximum force resulting from the instrumented indentation testing, after the selected maximum depth penetration, which is presented also. Rz roughness parameter values (determined after abrasive wear tests) are presented in order to compare with maximum depth penetration.

Table 2. Maximum penetration force F_{max} [N], maximum depth penetration h_{max} [μm] and Rz roughness parameter [μm].

Material	$F_{máx}$ [N]	h_{max} [μm]	Rz [μm]
AISI 1006	0.33 ± 0.01	3.2 ± 0.02	2.6 ± 0.4
Annealed AISI 52100	0.53 ± 0.02	3.02 ± 0.01	2.9 ± 0.6
Wire-drawing AISI 52100	0.743 ± 0.006	3.004 ± 0.005	2.9 ± 0.5
Quenched & tempered AISI 52100	0.94 ± 0.02	3.04 ± 0.02	3.3 ± 0.4

The comparison between h_{max} and Rz values shows that these values are very similar. As expected (Bulsara et al., 1998), the higher the material hardness, the higher F_{max} values.
Table 3 presents the α factor, calculated as shown in equation 9.

Table 3. α factor values.

Material	α (= 45.423 $h_{máx}^2$ / d^2)
AISI 1006	0.86
Annealed AISI 52100	0.90
Wire-drawing AISI 52100	0.95
Q & T AISI 52100	0.92

Following the Zeng et al. (1996) suggestion, AISI 1006 and AISI 52100 steel should be presented pilling-up after indentation tests, since α factor values were smaller than 1. This hypothesis was checked using laser interferometer, and it was verified that it was correct, as presented in Fig. 4 for wire-drawing AISI 52100 steel.

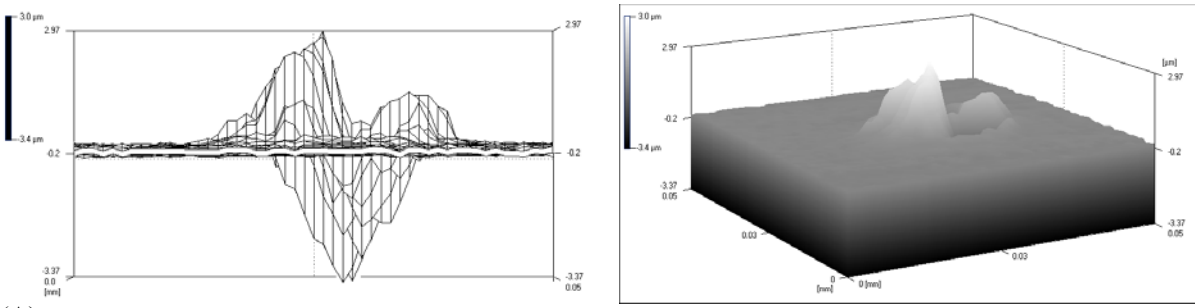

(A) (B)

Figure 4. Surface profile of wire-drawing AISI 52100 steel after indentation test: (A) transversal plane view and (B) 3D view.

One can be observe that Figure 4 is very similar to the result obtained by Alcalá et al. (2000), presented in Figure 2 (A), both for work-hardened materials.

Table 4 presents the values of the three kinds of hardness, based on the values presented in Tables 2 and 3., Figure 5 summarizes the results presented in Table 4, in order to facilitate the discussion.

Table 4. Vickers conventional hardness HV, Martens hardness HM and true hardness H_{IP} [GPa] of tested materials.

Material	HV (= 1,854 .$F_{máx}$ / d^2)	HM	H_{IP} (=α^2. $F_{máx}$ / 24,5.$h_{máx}^2$)
AISI 1006	1.15 ± 0.06	1.23 ± 0.060	0.99 ± 0.05
Annealed AISI 52100	2.15 ± 0.08	2.20 ± 0.06	1.93 ± 0.05
Wire-drawing AISI 52100	3.20 ± 0.05	3.11 ± 0.02	3.06 ± 0.02
Q & T AISI 52100	3.8 ± 0.1	3.83 ± 0.03	3.53 ± 0.03

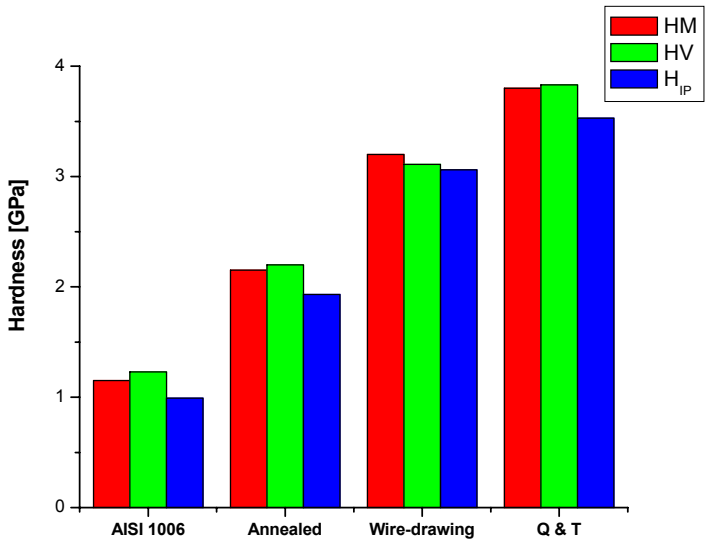

Figure 5. HM, HV e H_{IP} hardness values [GPa] of AISI 1006 and AISI 52100 steel.

Figure 5 shows that H_{IP} values are smaller than the other hardness values. This fact was expected taking into account the area that supports the applied force is large when the pilling-up effect is considered, because this morphology is associated with an increasing of plastic zone extension (Fig.2). Fig. 5 shows also that Martens hardness and conventional hardness values are similar for AISI 1006 and AISI 52100 steel. Therefore, it is possible to conclude that the indentation marks reflect the indenter geometry, since the elastic recovery is almost non existent and very small when measured by means of depth penetration.

Table 5 and Figure 6 present the α factor and hardness values of glass.

Table 5. Conventional Vickers, Martens and true hardness [GPa], α factor of glass.

Martens Hardness (HM)	3.25 ± 0.15
Conventional Vickers hardness (HV)*	5.5 ± 0.1
α factor*	1.57
True hardness (H_{IP})	8.6 ± 0.4

*these values were calculated based on a correction of indentation mark determined on MICROMET 2103 equipment using 0,98 N, due to the difference between this measurement and those determined using FISCHERSCOPE H100V equipment with 1 N.

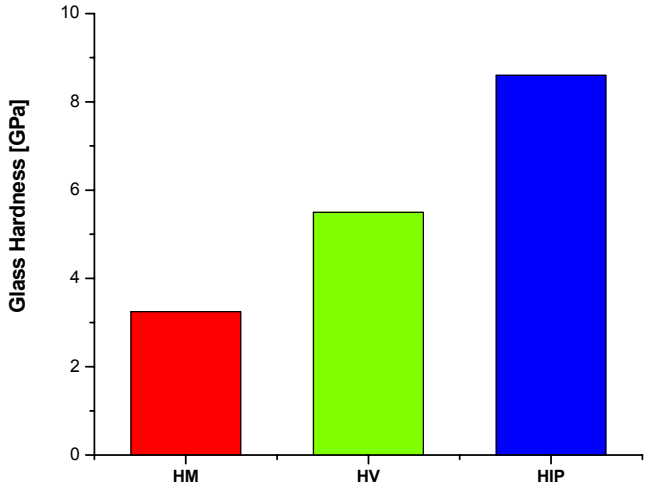

Figure 6. HM, HV e H_{IP} hardness values [GPa] of glass.

Figure 6 shows that the H_{IP} value of glass was significantly larger than the other hardness values. This result is a consequence of the reduction in the plastic zone extension, which happens in the cases of sinking-in occurrence. More than that and differently of what observed for AISI 1006 and AISI 52100 steel (Fig.4), the Martens hardness is very smaller than the conventional Vickers hardness values. This result means that, after removal of load, the indentation marks leaves to reflect the indenter geometry; due to the elastic recovery in depth penetration is very large (elastic work parcel is 63 ± 1 %), as presented schematically in Figure 7.

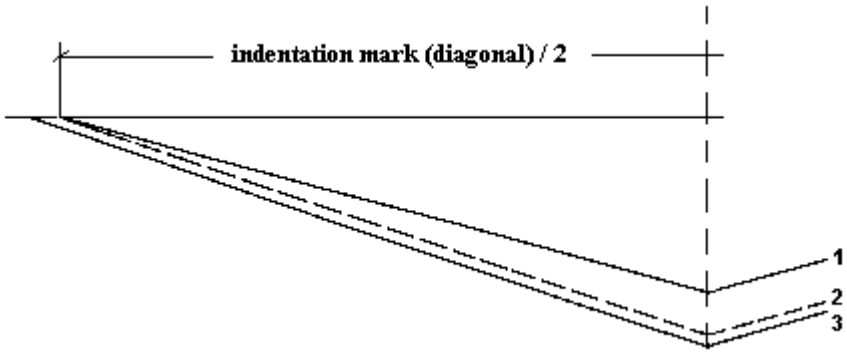

Figure 7. Sketch of depth penetration profiles possible to exist in a conventional Vickers testing (Weiler, 1989). Curve 1: real depth after removal of load; Curve 2: hypothetical depth, proportional to the recovery of diagonals; and Curve 3: depth under load application.

Figure 7 shows that the depth penetration after elastic recovery (curve 1) does not have geometric correspondence with the indentation mark due to the diagonal's elastic recovery be small or even be non existent.
Table 6 presents the α factor values following the proposals made by Giannakopoulos and Suresh (1996) and Alcalá et al. (2000).

Table 6. α factor of tested materials using Giannakopoulos and Suresh (1999) and Alcalá et al. (2000) proposals.

Material	Giannakopoulos and Suresh proposal: $(h_P / h_{máx})$	Alcalá et al. proposal: $(h_C / h_S)^2$
AISI 1006	0.95	43.9
Annealed AISI 52100	0.88	90.0
Wire-drawing AISI 52100	0.81	380.0
Q & T AISI 52100	0.80	143.8
Glass	0.45	1.5

*Note: the proposal made by Alcalá et al was calculated used the equation 11, as a result $\alpha_{alcalá} = \alpha_{zeng} / (\alpha_{zeng} - 1)$.

Table 6 shows that the proposal made by Giannakopoulos and Suresh (1999) did not work for the tested materials, since the α value should be larger than 0.875 to indicate pilling-up occurrence. Although AISI 1006 and AISI 52100 pilling-up was verified, it was found a value larger than 0.875 for AISI 1006. For glass, Giannakopoulos and Suresh proposal was able to preview the sinking-in occurrence, already confirmed in literature (Cook and Pharr, 1990). On the other hand, the proposal made by Alcalá et al. (2000) considers that pilling-up may occur if $\alpha^{1/2} - 1 > 0$. For AISI 1006 and AISI 52100 steel the values obtained from this expression are larger than 5, and for glass the calculated value is 0.2, showing a small deviation in relation of the expected value.

6. Implications of present results

In abrasive wear, the ratio between abrasive hardness and worn material hardness – H_A/H – is used to establish the wear severity of a pair of materials in a wear system. The wear severity increases as the H_A/H ratio increases. For H_A/H around 1.2 (Richardson, 1968), a wear transition from mild to severe abrasive wear can take place, if the hardness measurement of the materials is performed with conventional Vickers. Pintaúde et al. (2001b) verified that this threshold value depends on the testing load, because they found different H_A/H values using different testing loads for the same pair of tested materials.
In order to exemplify this assertive, Table 7 presents the H_A/H ratio obtained using the different kind of hardness (Tabs. 4 and 5 and Figs. 4 and 5), considering the quenched and tempered AISI 52100 steel as worn material and glass as an abrasive material.

Table 7. Ratios between abrasive hardness (glass, H_A) and hardness of quenched and tempered AISI 52100 steel (H), considering the following kind of hardness: Martens (HM), conventional Vickers (HV) and true hardness (H_{IP}).

Hardness	**H_A/H Ratio**
Martens (HM)	3.25 / 4.56 = 0.71
Conventional Vickers (HV)	5.50 / 4.55 = 1.21
True hardness (H_{IP})	8.60 / 4.21 = 2.04

Table 7 shows that the H_A/H ratio varies depends on the kind of hardness, which is considered. The changes on the H_A/H values are significant, especially due to the observed variation in the glass hardness, much larger than the variation on the steel hardness values. Therefore, if pilling-up or sinking-in occurrences are considered in abrasive wear phenomena, the use of classical criteria to define the transition between mild and severe wear regimes should be revised.

7. Conclusions

This paper proposes a new methodology to calculate the hardness of materials, called true hardness, H_{IP}. This concept take into account the pilling-up or sinking-in occurrences in indentation process. From the obtained results, it can be conclude:

- Materials with pilling-up occurrence have true hardness values smaller than the conventional Vickers hardness;
- For these materials, Martens hardness can be used as a good approximation of conventional Vickers hardness;
- Materials with sinking-in occurrence have true hardness values larger than the conventional Vickers hardness;

- The Zeng et al. (1996) proposal to preview indentation morphology can be used for the range of tested materials;
- The proposals made by Giannakopoulous and Suresh (1999) and by Alcalá et al. (2000) to preview the indentation morphologies (pilling-up or sinking-in) presented some distortions; and
- When pilling-up or sinking-in occurrences are considered in abrasive wear process, the ratio between abrasive hardness and worn material hardness changes from the conventional Vickers hardness.

8. Acknowledgments

Authors are very grateful to FAPESP – Sao Paulo Statement Agency for Research Financing, which support this work through 97/12621-5 and 00/10115-0 projects.

9. References

Alcalá, J.; Barone, A. C.; Anglada, M., 2000, "The influence of plastic hardening on surface deformation modes around Vickers and spherical indents", Acta Materialia, v. 48, pp. 3451-64.

Bulsara et al., 1998, "Mechanics of polishing", J. Applied Mechanics, v. 65, pp. 410-6.

Cook, R.F.; Pharr, G. M., 1990 , "Direct observation and analysis of indentation cracking in glasses and ceramics", J. of American Ceramic Soc., v. 73, pp. 787-817.

CSM INSTRUMENTS, 2002, Nanoindentation Reference Manual, Switzerland, 36 pp.

Doerner, M.F.; Nix, W. D., 1986, "A method for interpreting the data from depth-sensing indentation instruments", J. Mater. Research, v. 1, pp. 601-9.

Frölich, F.; Grau, P.; Grellmann, W., 1977, "Performance and analysis of recording microhardness tests", Physica Status Solidi A, v. 42, pp. 79-89.

Giannakopulos, A. E.; Suresh, S., 1999, "Determination of elastoplastic properties by instrumented sharp indentation", Scripta Materialia, v. 40, pp. 1191-8.

King, R. B., 1987, "Elastic analysis of some punch problems for a layered medium", Int. J. of Solids Structures, v. 23, pp. 1657-64.

ISO - International Organization for Standardization, 2002, ISO/FDIS 14577-1 - Metallic materials - Instrumented indentation test for hardness and material parameter - Part 1: Test method. Geneva, Switzerland.

Oliver, W.C., Pharr, G. M., 1992, "An improved technique for determining hardness and elastic modulus using load and displacement sensing indentation experiments", J. Mater. Res., v. 7, pp. 1564-83,.

Pintaude, G., Tanaka, D.K., Sinatora, A., 2001, "The influence of particle size and hardness of abrasive particles on the severity of two-body system" (in portuguese), Proceedings of the 16th Brazilian Congress of Mechanical Engineering, CD-ROM, Rio de Janeiro, Brazil.

Pintaude, G., Tanaka, D.K., Sinatora, A., 2001, "Effect of indentation size and microhardness calculation on abrasive wear severity abrasive wear regime", Scripta Materialia, v. 44, pp. 659-663.

Richardson, R.C.D., 1968, "The wear of metals by relatively soft abrasives", Wear, v. 11, pp. 245-75.

Strange, D. J.; Varshneya, A. K., 2001, "Finite element simulation of microindentation on aluminum", J. of Materials Science, v. 36, p. 1943-9,.

Weiler, W., 1989, "Hardness testing - a new method for economical and physically meaningful microhardness testing", The British J. of Non-Destructive Testing, v. 31, pp.253-8.

Wilde, H-R.; Wehrstedt, A., 2001, "Introduction of Martens Hardness HM", Materialprüfung, v. 42, pp. 468-470.

Zeng, K.; Söderlung, F.; Giannakopoulos, A. E.; Rowcliffe, D. J., 1996, "Controlled indentation: a general approach to determine mechanical properties of brittle materials", Acta Materialia, v. 44, pp. 1127-41.